MYCOLOGY
2025, VOL. 16, NO. 1, 369–381
https://doi.org/10.1080/21501203.2024.2354876

Taylor & Francis
Taylor & Francis Group

RESEARCH ARTICLE

OPEN ACCESS Check for updates

Mitochondrial phosphate carrier plays an important role in virulence of *Candida albicans*

Qiao-Ling Hu[a,b*], Hua Zhong[b*], Xin-Rong Wang[b], Lei Han[a], Shan-Shan Ma[b], Ling Li[b] and Yan Wang[a,b,c]

[a]School of Pharmacy, Fujian University of Traditional Chinese Medicine, Fuzhou, China; [b]School of Pharmacy, Second Military Medical University (Naval Medical University), Shanghai, China; [c]The Center for Fungal Infectious Diseases Basic Research and Innovation of Medicine and Pharmacy, Ministry of Education, Shanghai, China

ABSTRACT

Candida albicans is a common fungal pathogen that can cause life-threatening infections. *MIR1* is considered to be a mitochondrial phosphate carrier of *C. albicans*, while its role in virulence has not been fully elucidated. In this study, we found that *mir1Δ/Δ* mutant exhibited severe virulence defect in both nematode and murine models. Further mechanism studies revealed that the *mir1Δ/Δ* mutant grew more slowly than the wild-type strain and showed severe filamentation defects on the hypha-inducing agar media, including YPD + serum, Lee, Spider + glucose, SLAD, SLD, and YPS. Furthermore, the loss of *MIR1* resulted in unfermentable carbon utilisation defect, ATP decrease, and reactive oxygen species (ROS) accumulation in *C. albicans*. Antioxidant proanthocyanidins, vitamin E, and N-acetyl cysteine (NAC) could reduce intracellular ROS levels and partially rescue the filamentation defects of the *mir1Δ/Δ* mutant. Accordingly, hypha-specific genes, as well as *CEK1* and *RIM101* were down-regulated in the *mir1Δ/Δ* mutant, and this down-regulation could be partially rescued by the addition of the antioxidant NAC. Collectively, *MIR1* plays an important role in *C. albicans* mitochondrial function, filamentation and virulence, and would be a promising antifungal target.

ARTICLE HISTORY
Received 31 January 2024
Accepted 8 May 2024

KEYWORDS
Candida albicans; *MIR1*; reactive oxygen species; filamentation; virulence

1. Introduction

Fungi are widely distributed in nature with a wide variety of species, and some fungi can invade human tissues and organs, causing invasive fungal diseases (IFDs). IFDs are worldwide medical issues threatening human health and even life. In recent years, with chemotherapy for cancer patients, the widespread use of immunosuppressive drugs, the spread of viruses such as HIV and SARS-CoV-2, and the widespread use of broad-spectrum antibiotics, the morbidity and mortality of IFDs have increased dramatically (Chen et al. 2018; Gangneux et al. 2022; Li et al. 2022; Massart et al. 2023). A recent study showed that there are 6.5 million cases of invasive fungal infections each year, with 2.5 million deaths, or about 68% (Denning 2024). Of the pathogenic fungi that can cause disease in humans, *Candida* spp. is the most common (Chen et al. 2018; Bloos et al. 2022; Li et al. 2022). In 2022, the World Health Organization published for the first time a list of 19 fungal pathogens that posed a public health risk, with *Candida* being the most common fungal pathogen for life-threatening invasive infections (Fisher and Denning 2023). In clinical practice, it was found that the incidence of *Candida albicans* was dominant among all the *Candida* spp. (Brown et al. 2012). *C. albicans* infection occurs in 42.86% of catheter drainage patients, and diabetic and ICU patients are also at high risk for *C. albicans* infection (Li et al. 2022). It is also one of the most important causes of death in ICU patients (Chen et al. 2018).

The high morbidity of *C. albicans* infection is due to its high adaptability and virulence. *C. albicans* is a human commensal fungus, colonising mucosal surfaces such as oral, gastrointestinal, and genital tracts. When host immune function is compromised, *C. albicans* can be invasive and cause infections varying from superficial mucosal disorders to life-threatening bloodstream infections (Magill et al. 2014; Mylonakis et al. 2015; d'Enfert et al. 2021). Regarding its virulence trait, the yeast-hypha

CONTACT Yan Wang wangyansmmu@126.com; Hua Zhong zhonghuasmmu@hotmail.com School of Pharmacy, Second Military Medical University (Naval Medical University), 325 Guohe Road, Shanghai 200433, China

*These two authors contributed equally to this work.

This article has been republished with minor changes. These changes do not impact the academic content of the article.
Supplemental data for this article can be accessed online at https://doi.org/10.1080/21501203.2024.2354876

© 2024 The Author(s). Published by Informa UK Limited, trading as Taylor & Francis Group.
This is an Open Access article distributed under the terms of the Creative Commons Attribution-NonCommercial License (http://creativecommons.org/licenses/by-nc/4.0/), which permits unrestricted non-commercial use, distribution, and reproduction in any medium, provided the original work is properly cited. The terms on which this article has been published allow the posting of the Accepted Manuscript in a repository by the author(s) or with their consent.

morphological transition is vital. Studies have shown that *C. albicans* will change from the yeast state to the hyphal form after invading the host (Olivier et al. 2022). Thereby, inhibition of morphological transition is expected to be developed as a new antifungal strategy.

Along with the increased incidence of invasive fungal infections represented by *C. albicans* infections, the clinical application of antifungal drugs is also increasing. However, available drugs to treat fungal infections are very limited in clinics, mainly including azoles, polyenes, echinocandins, and nucleosides (Mota Fernandes et al. 2021). Accordingly, the antifungal targets that can be applied to develop drugs are also very limited. Azoles are known to target Erg11p (Wu et al. 2018), echinocandins to target Fas1p (Hu et al. 2023), flucytosine to target nucleic acid biosynthesis, and amphotericin B mainly to bind ergosterol in the cell membrane (Fisher et al. 2022). With the wide application of the available antifungal drugs, drug resistance has become a serious problem troubling the effect of clinical antifungal therapy (Mota Fernandes et al. 2021). Therefore, there is an urgent need for new antifungal treatment strategies, new drug targets, and new antifungal agents.

Targeting virulence factors is an effective strategy to fight fungal pathogens. To facilitate the study of *C. albicans* virulence, we have developed a *Caenorhabditis elegans*-based infection model that offers an efficient approach for high-throughput screening work and yeast-to-hypha transition studies (Tampakakis et al. 2008; Pukkila-Worley et al. 2009). Using this *C. elegans candidiasis* model, we found that a mutant lacking *MIR1* was significantly less virulent to *C. elegans*. *MIR1* encodes a putative mitochondrial phosphate transporter (http://www.candidagenome.org/), which is involved in phosphate transport and is associated with membrane potential and mitochondrial protein import (Zara et al. 1996).

In this study, we used the *mir1Δ/Δ* mutant and confirmed that it was avirulent in a murine candidiasis model and significantly hypo-virulent in the *C. elegans* model. The mechanism of this virulence defect was further explored.

2. Materials and methods

2.1. Strains and growth conditions

The *C. albicans* strains used in this study and the generation of the *mir1Δ/Δ* mutant, the *MIR1* re-integrated strain are described in our previous study (Xing et al. 2023). Strains were routinely grown in a YPD liquid medium (1% yeast extract, 2% peptone, and 2% dextrose) at 30 °C in a shaking incubator. Other medium used in this study included YPD + serum (YPD with 10% foetal calf serum), Lee's [1 L medium contains 0.5 g $(NH_4)_2SO_4$, 0.2 g $MgSO_4{\cdot}H_2O$, 0.25 g K_2HPO_4, 5 g NaCl, 0.0714 g ornithine, 0.5 g alanine, 1.3 g leucine, 1.0 g lysine, 0.5 g phenylalanine, 0.5 g proline, 0.5 g threonine, 0.1 g methionine, 0.001 g biotin, and 12.5 g dextrose], Spider (1% nutrient broth, 1% mannitol, and 0.2% K_2HPO_4), SLAD [2% dextrose and 0.17% YNB with 6.6 mg $(NH_4)_2SO_4$ per litre], SLD [0.2% dextrose, 0.17% YNB, and 0.5% $(NH_4)_2SO_4$, with 10 mg methionine per litre], and YPS (1% yeast extract, 2% peptone, and 2% sucrose).

2.2. Virulence assay using a C. elegans candidiasis model

C. elegans glp-4; sek-1 strain was propagated on nematode growth medium on lawns of *Escherichia coli* OP50 by using standard methods (Pukkila-Worley et al. 2009). Approximately 400 adult *C. elegans glp-4*; *sek-1* nematodes, synchronised in their development, were introduced into the middle of the *C. albicans* lawns placed on brain heart infusion (BHI) media. The setup was then incubated at a temperature of 25 °C for 4 h (Tan et al. 2014). Following a thorough wash, the worms were transferred using a pipette into a single well of a six-well tissue culture plate. This well contained 2 mL of liquid medium consisting of 80% M9 and 20% BHI, along with kanamycin at a concentration of 45 µg/mL. Any dead worms were counted daily.

2.3. Virulence assay using a murine candidiasis model

Mice were infected with *C. albicans* as described previously (Fuchs et al. 2010). ICR female mice (six-week-old, 18–22 g) were infected with 1.5×10^6 CFUs of *C. albicans* suspended in PBS via a tail vein injection in a 100 µL volume.

Two days after infection, the kidneys of the mice were removed aseptically, weighed and homogenised in sterile PBS. The dilutions were plated on YPD agar to determine the fungal burden of the kidneys.

Histopathological analysis was also performed to assess kidney damage. Kidney tissue was fixed in 10% neutral buffered formalin and embedded in paraffin. Thin sections were stained using periodic acid Schiff (PAS) to reveal the hyphal structure of the fungal pathogens (Wang et al. 2009).

2.4. Time-growth curve assay

The experiment was carried out as described previously with some modifications (Xu et al. 2017). The cells of WT, *mir1Δ/Δ*, and *mir1Δ/MIR1* were collected and then suspended in fresh YPD medium at a concentration of 1×10^6 cells/mL. Subsequently, the cells were cultured at a temperature of 30 °C while being continuously agitated at a speed of 200 r/min and the OD_{600} values were measured at designated time points after culture (0, 2, 4, 6, 8, 10, 12, and 24 h). The assay was carried out in triplicate.

2.5. Measurement of intracellular ethanol content

C. albicans cells were cultivated on Spider + glucose (100 mmol/L) at a temperature of 30 °C for 5 d, or on YPD + serum medium at a temperature of 37 °C for 3 d. The detection of ethanol content was carried out as previously described (Bi et al. 2018). 0.1–0.3 g cells were accurately weighted and suspended with 1 mL sterilised water. 700 µL glass beads (425–600 µm, Sigma) were added to each suspension, and the *C. albicans* cells were lysed by Bead Ruptor 12 (Omni 19-050A) and interrupted by cooling on ice. Glass beads were removed by centrifugation and the CheKine™ fluid ethanol kit (R-Biopharm AG) was utilised to measure the ethanol concentrations in the resulting supernatants. Triplicate independent experiments were conducted.

2.6. Measurement of intracellular ATP level

The measurement was performed as described previously with some modifications (Xu et al. 2009). Exponentially growing *C. albicans* cells were adjusted to 5×10^6 cells/mL and incubated at 30 °C in a shaking incubator for 30 min. Intracellular ATP was determined utilising the BacTiter-Glo reagent (BacTiter-Glo™ Microbial Cell Viability Assay, Promega, USA) and the signals were detected by a microplate reader (TECAN Infinite M200). To quantify the ATP levels, a standard curve was generated, and the ATP content was subsequently calculated based on this curve. The experiment was carried out in triplicate.

2.7. Measurement of intracellular ROS levels

The measurement was conducted as described previously (Sa et al. 2017). Exponentially growing strains were diluted to 1×10^6 cells/mL and incubated with 10 mmol/L of 2,7-dichlorofluorescin (DCFH-DA, Molecular Probes, Yeasen Biotechnology, China) at 30 °C, 200 r/min for 1 h to react with intracellular ROS. Then the probe was washed away and the samples were resuspended in a PBS buffer. The mean fluorescence intensity values were detected by flow cytometer (BD FACSCalibur) with excitation wavelength at 488 nm and the FL1 channel according to the product manuals. Triplicate independent experiments were conducted.

2.8. Measurement of mitochondrial ROS production rate

Mitochondrial ROS was detected by fluorescent probe DCFH-DA. *C. albicans* cells were adjusted to 5×10^6 cells/mL, and mitochondria were extracted using a working solution [CheKine™ Mitochondrial Reactive Oxygen Species (ROS) Production Rate Fluorometric Assay Kit, Abbkine, China] after wall-breaking in homogeniser. The extraction solution was incubated with fluorescent dye at 37 °C for 10 min, and the fluorescence values were recorded in 2 min by a microplate reader (TECAN Infinite M200) at the excitation wavelength of 488 nm and the emission wavelength of 525 nm. The mitochondrial ROS production rates of WT, *mir1Δ/Δ*, and *mir1Δ/MIR1* strains were calculated according to the formulas provided in the instructions.

2.9. RT-qPCR

Approximately 100 *C. albicans* cells were spread on a Spider + glucose agar plate [Spider +100 mmol/L glucose media containing 2% agar (Xu et al. 2015)]. Incubation was carried out at 37 °C for 3 d. Colonies were collected, washed and resuspended in DEPC-treated sterile ddH_2O. Total RNA was extracted using an RNA purification kit (Yeast Total RNA Isolation Kit, Sangon, China). The overall quality of RNA was determined by A_{260}/A_{280} and analysed by agarose gel

electrophoresis. For RT-qPCR assays, 500 ng of total RNA of each sample was used to synthesise cDNA with reverse transcriptase [5×PrimeScript RT Master Mix (Perfect Real Time), TaKaRa, China]. Independent reaction mixtures were carried out by the same cDNA template for both the genes of interest and the *ACT1* reference gene using the SYBR Green qPCR SuperMix [Hieff® qPCR SYBR Green Master Mix (No Rox), Yeasen, China] according to the instructions. The sequences of primers are shown in Table S1. The relative mRNA fold changes were determined by the $2^{-\Delta\Delta C_T}$ method using the CheKine™ 1 System. Data was shown in the form of log2. Triplicate independent experiments were conducted.

3. Results

3.1. *MIR1* is required for virulence of C. albicans

In this study, wild-type strain SC5314, a *mir1Δ/Δ* mutant, and a re-integrated strain *mir1Δ/MIR1* were used and we tested their virulence in two different infection models. In the *C. elegans* candidiasis model, the survival rate of the wild-type group was less than 40% within 48 h, and the survival rate dropped to approximately 20% at 120 h (Figure 1a), and each dead worm was visibly penetrated by hyphae through the cuticle (Figure 1b). Similar results were seen in the re-integrated strain group (Figure 1a,b). In contrast, the survival rate of the *mir1Δ/Δ* infection group remained at about 90% at 120 h, and no hyphae were observed in either alive or dead worms (Figure 1a,b). In the murine candidiasis model, the survival data indicated that the *mir1Δ/Δ* strain was non-lethal to mice during 21 days of observation, whereas the wild-type and the *mir1Δ/MIR1* strain killed all the hosts within 8 days (Figure 1c). The fungal burden in renal tissue was significantly lower in the *mir1Δ/Δ* mutant group than that in the wild-type group (Figure 1d, ***, $p < 0.001$). Periodic Acid Schiff (PAS) staining of the mouse kidneys showed that *C. albicans* hyphae were clustered after infection with the wild-type and *mir1Δ/MIR1* strains. However, no obvious hyphal cluster was observed in the *mir1Δ/Δ* infection group (Figure 1e). These results indicated that the *mir1Δ/Δ* mutant had a serious defect in virulence in both nematode and murine models.

3.2. *MIR1* is required for normal growth of C. albicans

To investigate how *MIR1* influences the virulence of *C. albicans* in the host, we tested several factors that contributed to the virulence of the fungal pathogen. First, we tested the influence of *MIR1* on the growth of the fungus *in vitro*. The results indicated that the wild-type and *mir1Δ/MIR1* strains showed a similar growth trend, while the *mir1Δ/Δ* mutant strain grew much slower than the wild-type and *mir1Δ/MIR1* strains in 24 h (Figure 2). The data demonstrated that *MIR1* is required for the growth of *C. albicans* and the deficiency of *MIR1* may slow down the growth process of the yeast.

3.3. *MIR1* affects hyphal formation of C. albicans

The morphogenetic change of *C. albicans* from yeast to hyphae facilitates invasion and plays an essential role in *C. albicans* virulence (Chen et al. 2020). In this study, we found that the *mir1Δ/Δ* mutant seemed to have hyphal defects in both nematode and murine models (Figure 1b,e), suggesting that *MIR1* might influence hyphal formation. Hence, hyphal formation was specifically investigated *in vitro* on agar systems mimicking features of tissue invasion (Kumamoto and Vinces 2005a, 2005b; Sudbery 2011). We incubated the wild-type, *mir1Δ/Δ*, and *mir1Δ/MIR1* strains on multiple hypha-inducing agar media under different temperatures (25, 30, and 37 °C) (Figure 3). The *mir1Δ/Δ* mutant did not grow on Spider (mannitol as carbon source) and displayed a severe filamentation defect on YPD + serum, Lee, Spider + glucose, SLAD (low nitrogen-containing medium), SLD (synthetic low dextrose medium), and YPS. More specifically, the *mir1Δ/Δ* mutant formed smooth-edged colonies on all the tested media (except for Spider) at various temperatures, in contrast to the wrinkled colonies or colonies with radial hyphae in the wild-type and the re-integrated strains (Figure 3). We also observed the hyphal formation of the *mir1Δ/Δ* mutant in liquid media. We cultured wild-type, *mir1Δ/Δ*, and *mir1Δ/MIR1* strains on four hypha-inducing liquid media at 37 °C. Interestingly, the *mir1Δ/Δ* mutant exhibited filamentation defects only in liquid Spider medium, but not in YPD + serum, Lee, or Spider + glucose (100 mmol/L) medium (Figure S1). Collectively, the results suggested that *MIR1* may play

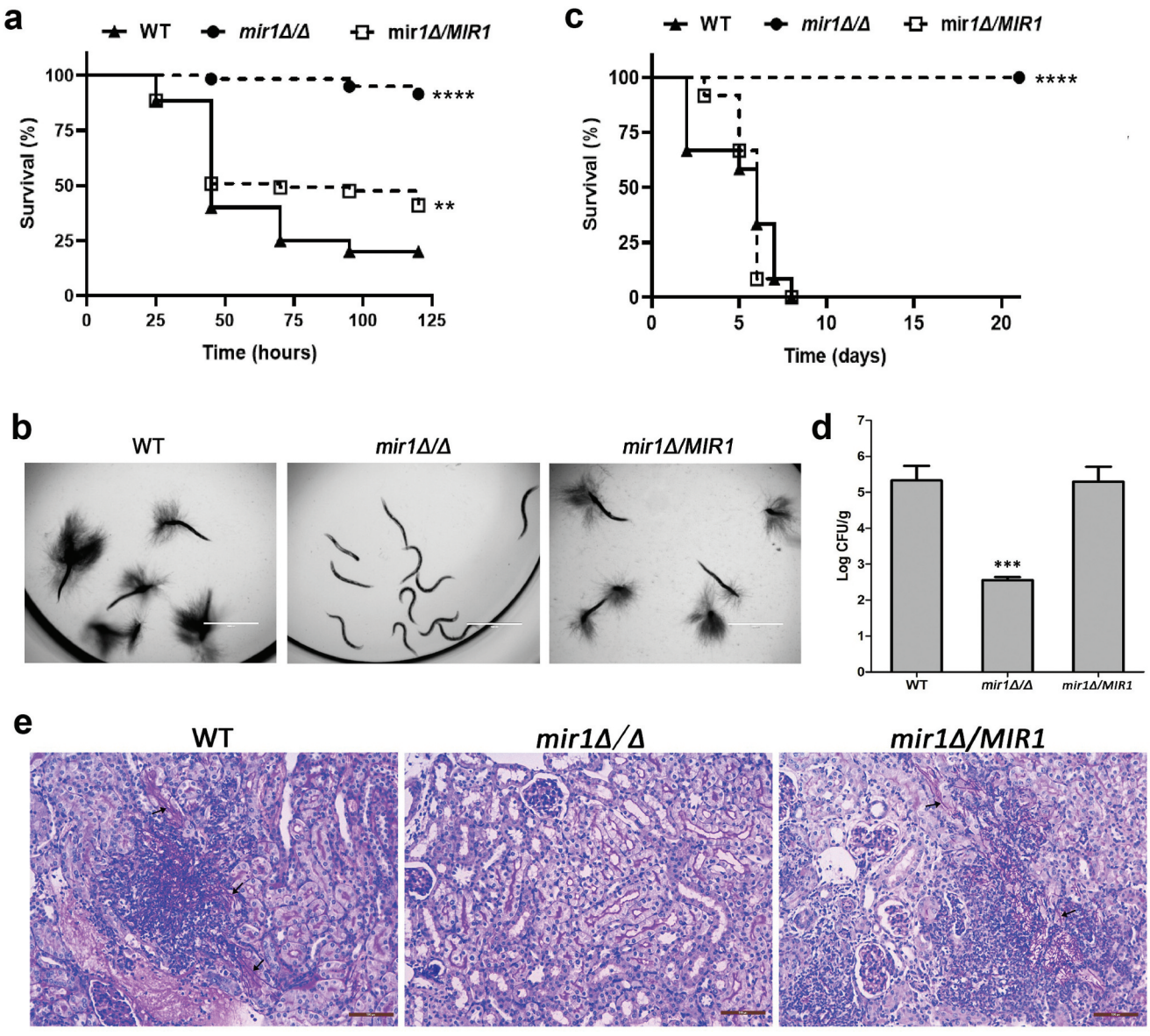

Figure 1. The *mir1Δ/Δ* mutant exhibited severe defects in virulence. (a) *Caenorhabditis elegans* survival was followed for 120 h after *Candida albicans* infection (60–70 worms per strain of *C. albicans*). **, $p < 0.01$, ****, $p < 0.0001$. (b) The *C. elegans* glp-4; sek-1 nematodes were infected by *C. albicans* wild-type, *mir1Δ/Δ*, or *mir1Δ/MIR1* strain, respectively. On day 3, the worms were photographed. Scale bars: 1 mm. (c) Mice survival was observed for 21 days. $n = 12$, ****, $p < 0.0001$. Mice were inoculated with 1.5×10^6 CFUs of the indicated strains intravenously and observed twice daily. (d) Fungal burden of the kidneys of mice infected with the wild-type, *mir1Δ/Δ*, or *mir1Δ/MIR1* strain, 2 days after inoculation. The data were analysed using one-way ANOVA followed by a *post hoc* Dunnett-*t* test. $n = 4$, ***, $p < 0.001$. (e) PAS stained thin sections of kidneys 2 days after inoculation with the indicated *C. albicans* strains. Tissues were examined by microscope. Arrows indicate *C. albicans* filaments in the tissues. These images were observed with an optical microscope at 400-fold magnification. Scale bars = 100 μm.

an important role in *C. albicans* filamentation features of tissue invasion.

To investigate whether *MIR1* influenced the filamentation on solid media by affecting budding in *C. albicans*, we examined the budding of *C. albicans* cells. It was observed that the absence of *MIR1* did not affect budding by comparing the wild-type, *mir1Δ/Δ*, and *mir1Δ/MIR1* strains in either liquid or solid media of Spider + glucose (100 mmol/L), and the budding rates of the wild-

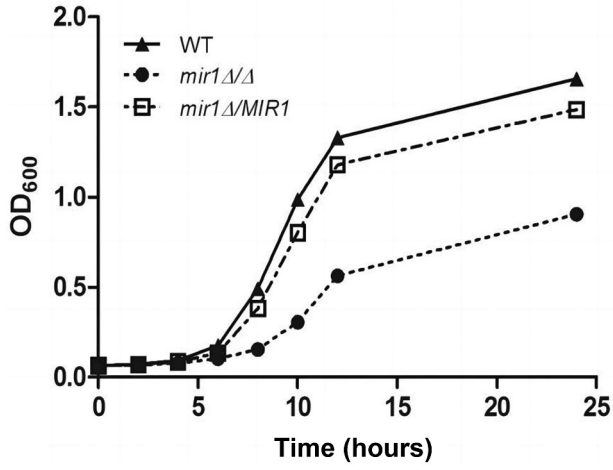

Figure 2. The growth curve of the wild-type, *mir1Δ/Δ*, and *mir1Δ/MIR1 Candida albicans* strains. Exponentially growing *C. albicans* cells were adjusted to 1×10^6 cells/mL, and cultured at 30 °C with constant shaking. The OD values were measured at designated time points.

type, *mir1Δ/Δ*, and *mir1Δ/MIR1* strain were almost the same in both media tested in this study (Figure S2).

3.4. MIR1 affects unfermentable carbon utilisation

As shown in Figure 3, the *mir1Δ/Δ* mutant could not grow on Spider agar, indicating a specific growth defect on the medium. Spider medium uses mannitol as the carbon source, which is non-fermentable, compared with other tested media. We then added glucose as a fermentable carbon source into Spider agar. We found that *mir1Δ/Δ* mutant could grow on Spider with glucose, but still could not form hyphae at 25, 30, and 37 °C compared with wild-type and *mir1Δ/MIR1* strains.

Based on these findings, we supposed that *MIR1* affected unfermentable carbon utilisation in *C. albicans*. To test the hypothesis, we incubated the three strains on YPG (with nonfermentable glycerol as a carbon source) and YPE (with nonfermentable ethanol as a carbon source) agar. The results showed that no obvious growth of the *mir1Δ/Δ* mutant could be observed after 24 h incubation at 30 °C on YPG or YPE agar (Figure 4a). Due to deficiencies in the ability to utilise non-fermentable carbon sources, the *mir1Δ/Δ* mutant might rely primarily on fermentative growth. Since ethanol is the main product in fermentation, we examined the amount of ethanol in the *mir1Δ/Δ* mutant cells. As expected, ethanol content in the *mir1Δ/Δ* mutant was significantly higher than in the wide-type strain in two different media (Figure 4b). As shown above, these results confirmed our hypothesis that *MIR1* played a role in unfermentable carbon utilisation in *C. albicans*.

3.5. Intracellular reactive oxygen species (ROS) accumulated in the mir1Δ/Δ mutant, leading to defects of hyphal formation

MIR1 encodes a putative mitochondrial phosphate carrier that catalyses the proton co-transport of phosphate into the mitochondrial matrix (Murakami et al. 1990; Phelps et al. 1991), which might affect the oxidative phosphorylation (Hamel et al. 2004). Consequently, the deficiency of *MIR1* might disturb ATP production and redox balance in mitochondria. Therefore, we measured intracellular ATP and ROS content to detect oxidative phosphorylation levels. As expected, the *mir1Δ/Δ* mutant showed decreased ATP concentration compared with the wild-type in YPD media (Figure 5a). The content of ATP in the *mir1Δ/Δ* mutant was 24.90 nmol/L, which was about 1/3 of the content in the wild-type strain. Moreover, the redox balance was interrupted in the *mir1Δ/Δ* mutant. Our results indicated that the intracellular ROS level increased by about 2.5 times (Figure 5b), and the mitochondrial ROS production rate increased by about 2 times in the *mir1Δ/Δ* mutant strain (Figure 5c) compared with the wild-type strain, indicating that the ROS accumulated in the *mir1Δ/Δ* mutant, and the ROS accumulation was in accordance with the mitochondrial ROS production rate.

Furthermore, we examined whether the accumulated intracellular ROS level was associated with the hyphal growth defects in the *mir1Δ/Δ* mutant strain. We used antioxidants to reduce the intracellular ROS levels in the *mir1Δ/Δ* mutant strain and observed the hyphal growth. All the 3 antioxidants used in this study, including proanthocyanidins, vitamin E, and N-acetyl cysteine (abbreviated as PC, VE, and NAC, respectively) could significantly reduce the intracellular ROS levels in the *mir1Δ/Δ* mutant strain (Figure 5d, ***, $p < 0.001$ or ****, $p < 0.0001$). Then the 3 antioxidants were added to the hyphal-inducing media respectively to observe their effects on the filamentation of the *mir1Δ/Δ* mutant strain. The results indicated that adding 600 μmol/L PC,

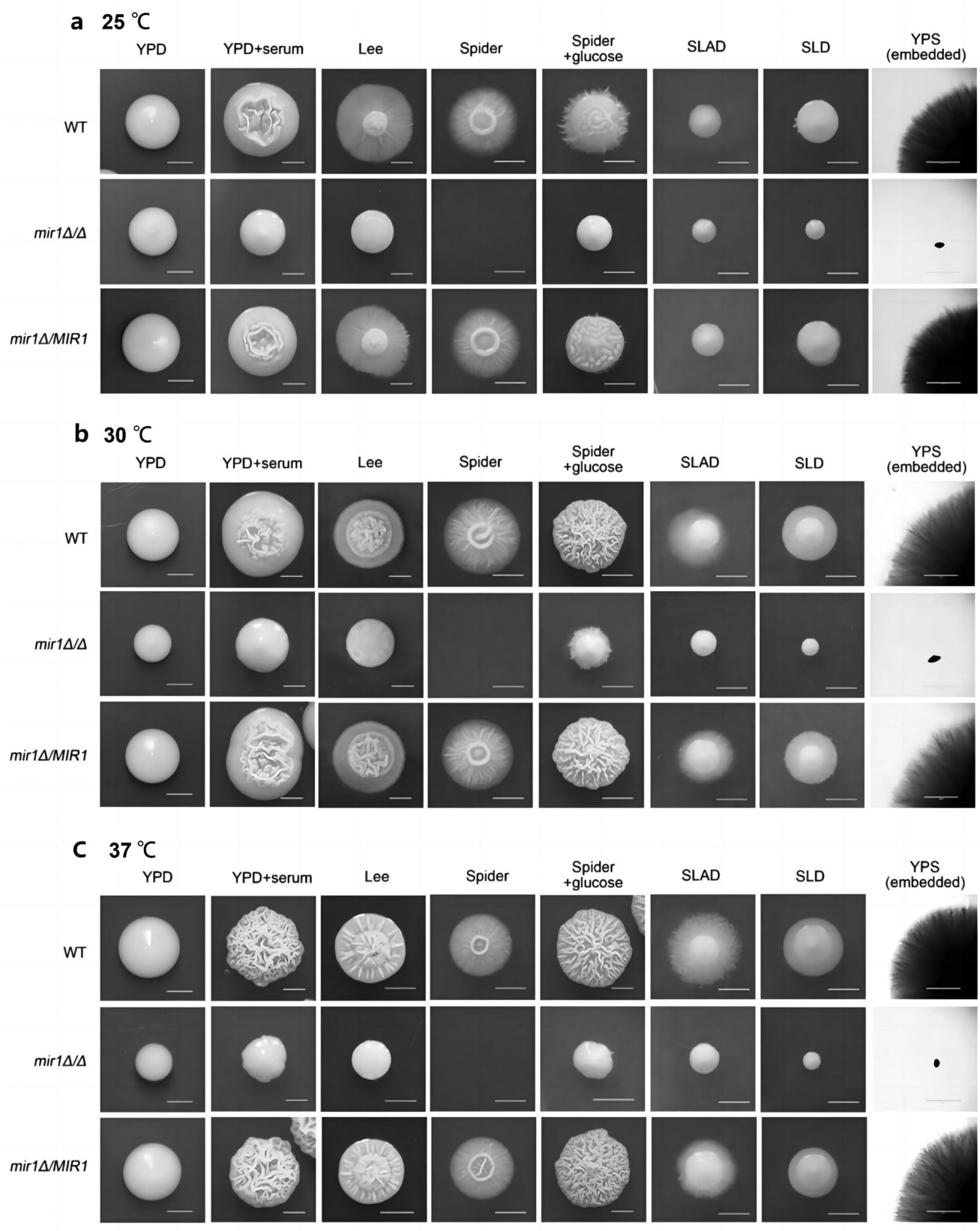

Figure 3. The *mir1Δ/Δ* mutant strain could not form hyphae on many kinds of media. Hyphal formation of *Candida albicans* wild-type, *mir1Δ/Δ*, and *mir1Δ/MIR1* strains on different media at (a) 25 °C, (b) 30 °C, (c) 37 °C. Scale bars = 1 mm.

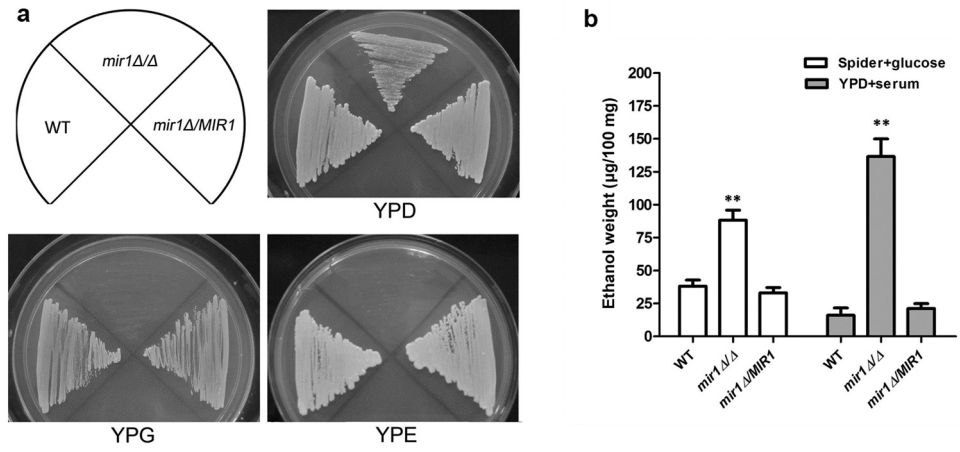

Figure 4. *MIR1* affects unfermentable carbon utilisation in *Candida albicans*. (a) The *mir1Δ/Δ* mutant couldn't grow on nonfermentable carbon sources. YPD: Contains fermentable glucose as the carbon source; YPG: Contains nonfermentable glycerol as the carbon source; YPE: Contains nonfermentable ethanol as the carbon source. (b) The ethanol content in *C. albicans* wild-type, *mir1Δ/Δ*, and *mir1Δ/MIR1* strains growing in spider + glucose or YPD + serum. **, $p < 0.01$.

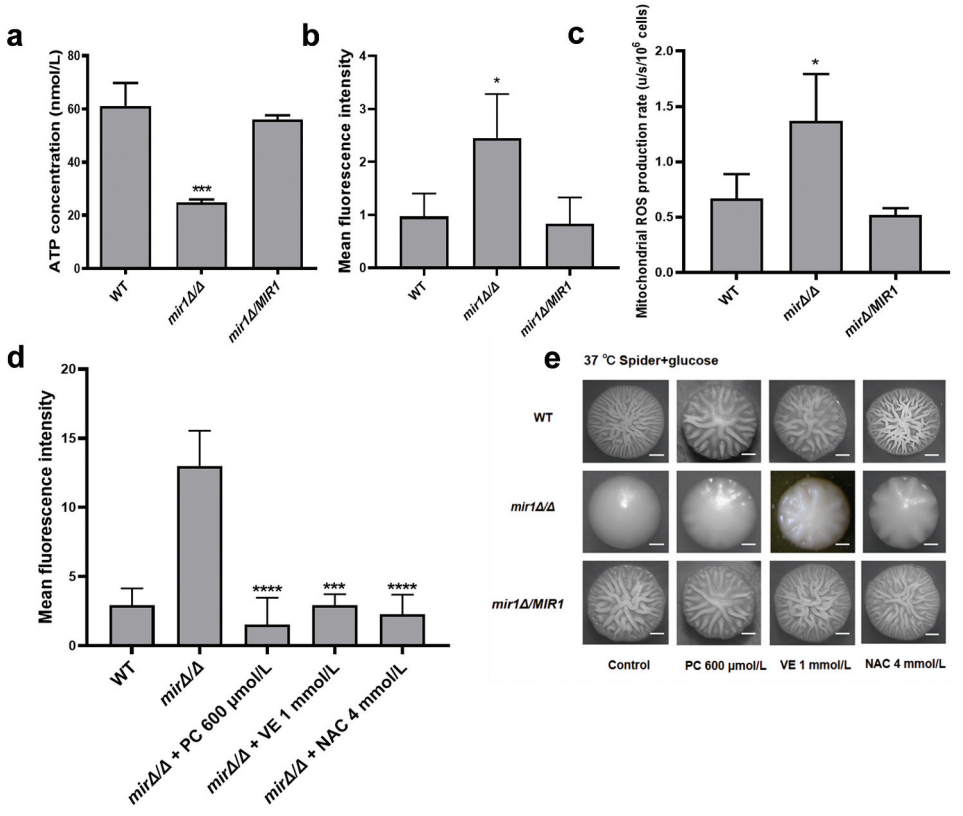

Figure 5. Intracellular reactive oxygen species (ROS) accumulated in the *mir1Δ/Δ* mutant, leading to hyphal formation defects. (a) The ATP content of *Candida albicans* wild-type, *mir1Δ/Δ*, and *mir1Δ/MIR1* strains. ***, $p < 0.001$. (b) The intracellular ROS content of *C. albicans* wild-type, *mir1Δ/Δ*, and *mir1Δ/MIR1* strains. *, $p < 0.05$. (c) The mitochondrial ROS production rate of *C. albicans* wild-type, *mir1Δ/Δ*, and *mir1Δ/MIR1* strains. *, $p < 0.05$ compared with the wild-type strain. (d) Effect of antioxidants on intracellular ROS levels of wild-type strain and *mir1Δ/Δ* mutant. 600 μmol/L proanthocyanidins (PC), 1 mmol/L vitamin E (VE), and 4 mmol/L N-acetyl cysteine (NAC) were added into YPD medium respectively, strains were incubated at 30 °C for 1 h. ***, $p < 0.001$; ****, $p < 0.0001$. (e) Effect of antioxidants on filamentation of *C. albicans* wild-type, *mir1Δ/Δ*, and *mir1Δ/MIR1* strains. 600 μmol/L PC, 1 mmol/L VE, and 4 mmol/L NAC were added into spider + glucose solid medium respectively. Plates were incubated at 30 °C for 7 d. Scale bars = 1 mm.

1 mmol/L VE, or 4 mmol/L NAC to the agar partially rescued the filamentation defects of the *mir1Δ/Δ* mutant strain (Figure 5e). In contrast to the smooth edges of the control *mir1Δ/Δ* mutant colonies, the colonies grown on the antioxidant-added agar were significantly wrinkled. These results demonstrated that the functional defect of *MIR1* led to intracellular ROS accumulation, which in turn influenced filamentation in the *mir1Δ/Δ* mutant strain. Reducing the ROS level in cells partially restored this hyphal formation defect.

3.6. Cek MAPK pathway and Rim101 pathway might be involved in the hyphal formation defects of the mir1Δ/Δ mutant

To explore whether the hyphal formation defect in the *mir1Δ/Δ* mutant was due to the blockage of hyphal-related signalling pathways, we performed RT-qPCR. In the *mir1Δ/Δ* mutant, *CEK1* and *RIM101* were obviously down-regulated, meanwhile, the hypha-specific genes *ECE1*, *HYR1*, and *HWP1* were also down-regulated (Figure 6a). We also investigated the effects of the antioxidant on the hyphal-related gene expression in the *mir1Δ/Δ* mutant. The results showed that the antioxidant NAC could rescue the down-regulation of hypha-specific genes, as well as *CEK1* and *RIM101* (Figure 6b). These findings suggested that the hyphal formation defect of the *mir1Δ/Δ* mutant might be related to the obstruction of the Cek MAPK pathway and Rim101 pathway, leading to the downregulation of downstream hypha-specific genes, and resulting in hyphal formation defects.

4. Discussion

In *Saccharomyces cerevisiae*, *MIR1* encodes a mitochondrial phosphate carrier that is involved in the proton co-transport of phosphate into the mitochondrial matrix (Murakami et al. 1990; Zara et al. 1996). In the present study, we revealed a novel role of *MIR1* in *C. albicans* virulence and found that the deletion of *MIR1* markedly attenuated the virulence of *C. albicans* in both the *C. elegans* and the murine candidiasis models. A prominent reason for the loss of virulence is the dramatic defect in the yeast-to-hypha transition of the *mir1Δ/Δ* mutant. The hyphal formation is an important attribute in *C. albicans* virulence. Mutants that are unable to form hyphae are reported to be avirulent (Lo et al. 1997; Bi et al. 2018). In this study, the *mir1Δ/Δ* mutant could not form hyphae to puncture the nematode or cluster in the kidneys of mice, and it showed severe filamentation defects in all tested hypha-inducing media. The defect in the yeast-to-hypha transition may contribute to the attenuated virulence of the *mir1Δ/Δ* mutant. Furthermore, this morphological transformation defect is associated with mitochondrial dysfunction and ROS accumulation. Antioxidants could eliminate intracellular ROS and rescue filamentation defects. Furthermore, the Cek MAPK pathway and Rim101 pathway may be involved in the filamentation defects of the *mir1Δ/Δ* mutant. Overall, this study suggests that *MIR1* plays a vital role in respiration, filamentation and virulence of *C. albicans*, and disrupting respiration through blocking the mitochondrial phosphate carrier may serve as a potent antifungal strategy.

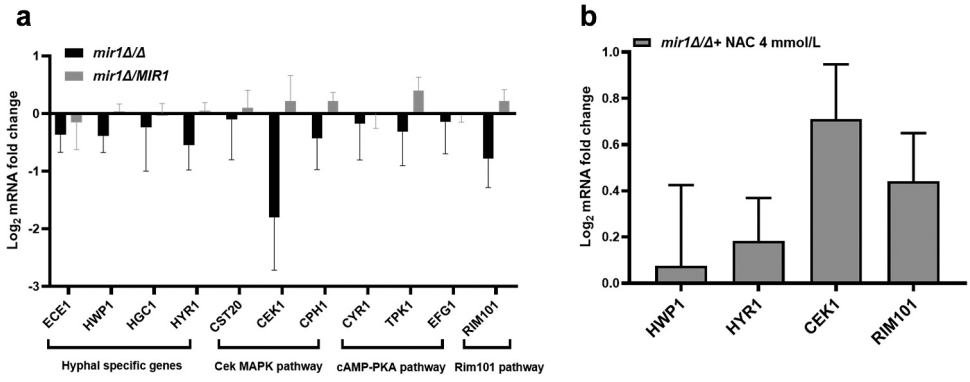

Figure 6. The Cek MAPK pathway and Rim101 pathway might be involved in the hyphal formation defects of the *mir1Δ/Δ* mutant. Cells grown on spider + glucose (100 mmol/L) agar medium for 3 days were harvested and used for mRNA extraction. To investigate the effect of antioxidants, spider + glucose (100 mmol/L) agar medium was added with 4 mmol/L NAC. Expression levels of the selected genes were assessed by RT-qPCR. (a) Relative mRNA levels of some hypha-related genes in *Candida albicans* wild-type, *mir1Δ/Δ*, and *mir1Δ/MIR1* strains. (b) Effect of the antioxidant NAC on the mRNA levels of some hypha-related genes in the *mir1Δ/Δ* mutant.

There are two ways of energy production in *C. albicans* cells, fermentation and respiration. Fermentation pathways can ferment carbohydrates to ethanol and produce ATP in the process. Respiration is more efficient in ATP production since carbohydrates can be thoroughly metabolised into water and carbon dioxide in this strategy. *C. albicans* prefers respiration in most cases when oxygen is sufficient (Askew et al. 2009). Of note, the *mir1Δ/Δ* mutant exhibited a respiration defect, as evidenced by its defect in utilising non-fermentable carbon sources. This may be explained by the insufficient supply of phosphate caused by *MIR1* dysfunction since it is one of the key substrates in ATP production (Murakami et al. 1990). The *mir1Δ/Δ* mutant failed to form hyphae. This may indicate that respiration is essential for the filamentation of *C. albicans*.

Respiration is composed of a series of metabolic processes including glycolysis, tricarboxylic acid (TCA) cycle, and adenosine triphosphate (ATP) synthesis via oxidative phosphorylation (Duvenage et al. 2019). Goa1 protein is required for respiratory growth and mutants that lack Goa1 are compromised in hyphal growth and avirulent in a murine model of haematogenous disseminated candidiasis (Bambach et al. 2009). Further study shows that interrupting *DPB4* and *RBF1*, which are the transcriptional regulators of *GOA1*, also affects the yeast-to-hyphal transition of *C. albicans* (Khamooshi et al. 2014). Previously, we revealed that lacking iron-sulphur subunit of succinate dehydrogenase (also named respiratory complex II) leads to both filamentation and virulence defects (Bi et al. 2018). In this study, we further revealed that lacking mitochondrial phosphate carriers leads to severe filamentation and virulence defects. Collectively, it can be inferred that respiration is associated with virulence of *C. albicans* and intervention in respiration of pathogenic fungi may become an antifungal strategy.

ROS is a bunch of active substances containing unpaired electrons derived from O_2, such as $\cdot O_2$, H_2O_2, and ·OH (Halliwell and Gutteridge 2007). It is mainly produced by mitochondria in *C. albicans* cells. When the function of mitochondria is disturbed, ROS may accumulate and lead to cell damage. Excessive ROS can break the DNA chains and damage proteins, resulting in cell apoptosis and cell death (Dwyer et al. 2012; Foti et al. 2012). Our previous study has clarified that the increased intracellular ROS is associated with the filamentation defects of *C. albicans*. The ROS-inducing agents could inhibit the hyphal growth of the yeast in a dose-dependent manner (Bi et al. 2018). In this study, lack of *MIR1* led to mitochondria dysfunction and ROS accumulation in *C. albicans*. This may contribute to the growth and filamentation defects in the fungal cells. Meanwhile, antioxidants such as PC, VE, and NAC, could decrease ROS levels in cells and restore the hyphal formation ability. These experiments confirmed that ROS is associated with filamentation defects in *C. albicans*, and accumulating intracellular ROS by influencing respiration is a promising antifungal strategy.

Hypha-specific genes, including *ECE1*, *HWP1*, *HGC1*, and *HYR1*, affect *C. albicans* hyphal formation (Silva et al. 2017). They are downstream genes regulated by several signalling pathways. The Cek MAPK pathway, for example, is induced by the embedding matrix environment, cell wall damage and low nitrogen. The signals are transmitted from *CST20* to *CEK1* through *STE11* and *HST7*, and eventually lead to hyphal formation through phosphorylation of transcription factors *CPH1* (Chen et al. 2020). While regarding the cAMP-PKA pathway, *CYR1*-encoded adenylate cyclase can increase the synthesis of cAMP, thereby activating the cAMP-dependent protein kinase regulatory subunits, and then activating the catalytic subunit *TPK1*. *TPK1* activates *EFG1*, upregulates hypha-specific genes, and induces hyphal formation, which contributes to filaments on solid media (Giacometti et al. 2011). Besides, there is also a pH-sensing pathway regulating hyphal formation, mainly mediated by Rim101 (Li et al. 2004). In this study, *MIR1* deletion resulted in hyphal defects in *C. albicans*. It seemed that the hyphal defects caused by *MIR1* deletion might be partially due to the inhibition of the *CEK1*-mediated Cek MAPK pathway and Rim101-mediated pH signalling pathway, rather than the cAMP-PKA pathway. Meanwhile, antioxidant NAC could partially restore the expression of the hypha-specific genes in the *mir1Δ/Δ* mutant, which is

consistent with the results of hyphal formation. Nevertheless, more evidence is still needed to validate the role of the Cek MAPK pathway and Rim101 pathway in the hyphal formation of the *mir1Δ/Δ* mutant.

Disclosure statement

No potential conflict of interest was reported by the author(s).

Funding

This work was supported by the Biosafety Program [20SWAQX29-1-6, 145AHQ082021000X] and the National Natural Science Foundation of China [82204470, 82104127].

Author contributions

Qiao-Ling Hu: Investigation, writing original draft, formal analysis. **Hua Zhong**: Methodology, writing original draft, visualisation, funding acquisition. **Xin-Rong Wang**: Investigation. **Lei Han**: Investigation. **Shanshan Ma**: Investigation. **Ling Li**: Investigation, funding acquisition. **Yan Wang**: Conceptualization, investigation, resources, supervision, funding acquisition.

Ethical approval

The murine protocol was approved by the Committee on Ethic of Medical Research, Naval Medical University.

References

Askew C, Sellam A, Epp E, Hogues H, Mullick A, Nantel A, Whiteway M. 2009. Transcriptional regulation of carbohydrate metabolism in the human pathogen *Candida albicans*. PLoS Pathog. 5(10):e1000612. doi: 10.1371/journal.ppat.1000612.

Bambach A, Fernandes MP, Ghosh A, Kruppa M, Alex D, Li D, Fonzi WA, Chauhan N, Sun N, Agrellos OA, et al. 2009. Goa1p of *Candida albicans* localizes to the mitochondria during stress and is required for mitochondrial function and virulence. Eukaryot Cell. 8(11):1706–1720. doi: 10.1128/ec.00066-09.

Bi S, Lv QZ, Wang TT, Fuchs BB, Hu DD, Anastassopoulou CG, Desalermos A, Muhammed M, Wu CL, Jiang YY, et al. 2018. SDH2 is involved in proper hypha formation and virulence in *Candida albicans*. Future Microbiol. 13(10):1141–1156. doi: 10.2217/fmb-2018-0033.

Bloos F, Held J, Kluge S, Simon P, Kogelmann K, de Heer G, Kuhn SO, Jarczak D, Motsch J, Hempel G, et al. 2022. (1 → 3)-β-D-Glucan-guided antifungal therapy in adults with sepsis: the CandiSep randomized clinical trial. Intensive Care Med. 48(7):865–875. doi: 10.1007/s00134-022-06733-x.

Brown GD, Denning DW, Gow NA, Levitz SM, Netea MG, White TC. 2012. Hidden killers: human fungal infections. Sci Transl Med. 4(165):165rv13. doi: 10.1126/scitranslmed.3004404.

Chen H, Zhou X, Ren B, Cheng L. 2020. The regulation of hyphae growth in *Candida albicans*. Virulence. 11(1):337–348. doi: 10.1080/21505594.2020.1748930.

Chen M, Xu Y, Hong N, Yang Y, Lei W, Du L, Zhao J, Lei X, Xiong L, Cai L, et al. 2018. Epidemiology of fungal infections in China. Front Med. 12(1):58–75. doi: 10.1007/s11684-017-0601-0.

d'Enfert C, Kaune AK, Alaban LR, Chakraborty S, Cole N, Delavy M, Kosmala D, Marsaux B, FróFróIs-Martins R, Morelli M, et al. 2021. The impact of the fungus-host-microbiota interplay upon *Candida albicans* infections: current knowledge and new perspectives. FEMS Microbio Rev. 45(3):fuaa060. doi: 10.1093/femsre/fuaa060.

Denning DW. 2024. Global incidence and mortality of severe fungal disease. Lancet Infect Dis. 12:S1473–3099(23)00692–8. doi: 10.1016/S1473-3099(23)00692-8.

Duvenage L, Walker LA, Bojarczuk A, Johnston SA, MacCallum DM, Munro CA, Gourlay CW, Traven A, Berman J. 2019. Inhibition of classical and alternative modes of respiration in *Candida albicans* leads to cell wall remodeling and increased macrophage recognition. Mbio. 10(1):e02535–18. doi: 10.1128/mBio.02535-18.

Dwyer DJ, Camacho DM, Kohanski MA, Callura JM, Collins JJ. 2012. Antibiotic-induced bacterial cell death exhibits physiological and biochemical hallmarks of apoptosis. Mol Cell. 46(5):561–572. doi: 10.1016/j.molcel.2012.04.027.

Fisher MC, Alastruey-Izquierdo A, Berman J, Bicanic T, Bignell EM, Bowyer P, Bromley M, Brüggemann R, Garber G, Cornely OA, et al. 2022. Tackling the emerging threat of antifungal resistance to human health. Nat Rev Microbiol. 20(9):557–571. doi: 10.1038/s41579-022-00720-1.

Fisher MC, Denning DW. 2023. The WHO fungal priority pathogens list as a game-changer. Nat Rev Microbiol. 21(4):211–212. doi: 10.1038/s41579-023-00861-x.

Foti JJ, Devadoss B, Winkler JA, Collins JJ, Walker GC. 2012. Oxidation of the guanine nucleotide pool underlies cell death by bactericidal antibiotics. Science. 336(6079):315–319. doi: 10.1126/science.1219192.

Fuchs BB, Eby J, Nobile CJ, El Khoury JB, Mitchell AP, Mylonakis E. 2010. Role of filamentation in *Galleria mellonella* killing by *Candida albicans*. Microbes Infect. 12(6):488–496. doi: 10.1016/j.micinf.2010.03.001.

Gangneux JP, Dannaoui E, Fekkar A, Luyt CE, Botterel F, De Prost N, Tadié JM, Reizine F, Houzé S, Timsit JF, et al. 2022. Fungal infections in mechanically ventilated patients with COVID-19 during the first wave: the French multicentre MYCOVID study. Lancet Respir Med. 10(2):180–190. doi: 10.1016/S2213-2600(21)00442-2.

Giacometti R, Kronberg F, Biondi RM, Passeron S. 2011. Candida albicans Tpk1p and Tpk2p isoforms differentially regulate pseudohyphal development, biofilm structure, cell aggregation and adhesins expression. Yeast. 28(4):293–308. doi: 10.1002/yea.1839.

Halliwell B, Gutteridge JMC. 2007. Free radicals in biology and medicine. 4th ed. Oxford (UK): Oxford University Press. doi: 10.1093/acprof:oso/9780198717478.001.0001.

Hamel P, Saint-Georges Y, de Pinto B, Lachacinski N, Altamura N, Dujardin G. 2004. Redundancy in the function of mitochondrial phosphate transport in *Saccharomyces cerevisiae* and *Arabidopsis thaliana*. Mol Microbiol. 51 (2):307–317. doi: 10.1046/j.1365-2958.2003.03810.x.

Hu X, Yang P, Chai C, Liu J, Sun H, Wu Y, Zhang M, Zhang M, Liu X, Yu H. 2023. Structural and mechanistic insights into fungal β-1, 3-glucan synthase FKS1. Nature. 616 (7955):190–198. doi: 10.1038/s41586-023-05856-5.

Khamooshi K, Sikorski P, Sun N, Calderone R, Li D. 2014. The Rbf1, Hfl1 and Dbp4 of *Candida albicans* regulate common as well as transcription factor-specific mitochondrial and other cell activities. BMC Genomics. 15(1):56. doi: 10.1186/1471-2164-15-56.

Kumamoto CA, Vinces MD. 2005a. Alternative *Candida albicans* lifestyles: growth on surfaces. Annu Rev Microbiol. 59 (1):113–133. doi: 10.1146/annurev.micro.59.030804.121034.

Kumamoto CA, Vinces MD. 2005b. Contributions of hyphae and hypha-co-regulated genes to *Candida albicans* virulence. Cell Microbio. 7(11):1546–1554. doi: 10.1111/j.1462-5822.2005.00616.x.

Li M, Martin SJ, Bruno VM, Mitchell AP, Davis DA. 2004. *Candida albicans* Rim13p, a protease required for Rim101p processing at acidic and alkaline pHs. Eukaryot Cell. 3(3):741–751. doi: 10.1128/EC.3.3.741-751.2004.

Li XV, Leonardi I, GG P, Semon A, Fiers WD, Kusakabe T, WY L, IH G, Doron I, Gutierrez-Guerrero A, et al. 2022. Immune regulation by fungal strain diversity in inflammatory bowel disease. Nature. 603(7092):672–678. doi: 10.1038/s41586-022-04502-w.

Li Y, Wu Y, Gao Y, Niu X, Li J, Tang M, Fu C, Qi R, Song B, Chen H, et al. 2022. Machine-learning based prediction of prognostic risk factors in patients with invasive candidiasis infection and bacterial bloodstream infection: a singled centered retrospective study. BMC Infect Dis. 22(1):150. doi: 10.1186/s12879-022-07125-8.

Lo HJ, Kohler JR, DiDomenico B, Loebenberg D, Cacciapuoti A, Fink GR. 1997. Nonfilamentous *C. albicans* mutants are avirulent. Cell. 90(5):939–949. doi: 10.1016/s0092-8674(00)80358-x.

Magill SS, Edwards JR, Bamberg W, Beldavs ZG, Dumyati G, Kainer MA, Lynfield R, Maloney M, McAllister-Hollod L, Nadle J, et al. 2014. Multistate point-prevalence survey of health care-associated infections. N Engl J Med. 370 (13):1198–1208. doi: 10.1056/NEJMoa1306801.

Massart N, Reizine F, Dupin C, Legay F, Legris E, Cady A, Rieul G, Barbarot N, Magahlaes E, Fillatre P. 2023. Prevention of acquired invasive fungal infection with decontamination regimen in mechanically ventilated ICU patients: a pre/post observational study. Infect Dis (Lond). 55(4):263–271. doi: 10.1080/23744235.2023.2170460.

Mota Fernandes C, Dasilva D, Haranahalli K, McCarthy JB, Mallamo J, Ojima I, Del Poeta M. 2021. The future of antifungal drug therapy: novel compounds and targets. Antimicrob Agents Chemother. 65(2):e01719-20. doi: 10.1128/AAC.01719-20.

Murakami H, Blobel G, Pain D. 1990. Isolation and characterization of the gene for a yeast mitochondrial import receptor. Nature. 347(6292):488–491. doi: 10.1038/347488a0.

Mylonakis E, Clancy CJ, Ostrosky-Zeichner L, Garey KW, Alangaden GJ, Vazquez JA, Groeger JS, Judson MA, Vinagre YM, Heard SO, et al. 2015. T2 magnetic resonance assay for the rapid diagnosis of candidemia in whole blood: a clinical trial. Clin Infect Dis. 60(6):892–899. doi: 10.1093/cid/ciu959.

Olivier FAB, Hilsenstein V, Weerasinghe H, Weir A, Hughes S, Crawford S, Vince JE, Hickey MJ, Traven A. 2022. The escape of *Candida albicans* from macrophages is enabled by the fungal toxin candidalysin and two host cell death pathways. Cell Rep. 40(12):111374. doi: 10.1016/j.celrep.2022.111374.

Phelps A, Schobert CT, Wohlrab H. 1991. Cloning and characterization of the mitochondrial phosphate transport protein gene from the yeast *Saccharomyces cerevisiae*. Biochemistry. 30(1):248–252. doi: 10.1021/bi00215a035.

Pukkila-Worley R, Peleg AY, Tampakakis E, Mylonakis E. 2009. *Candida albicans* hyphal formation and virulence assessed using a *Caenorhabditis elegans* infection model. Eukaryot Cell. 8(11):1750–1758. doi: 10.1128/EC.00163-09.

Sa NP, Lima CM, Lino CI, Barbeira PJS, Baltazar LM, Santos DA, Oliveira RB, Mylonakis E, Fuchs BB, Johann S. 2017. Heterocycle thiazole compounds exhibit antifungal activity through increase in the production of reactive oxygen species in the *Cryptococcus neoformans-Cryptococcus gattii* species complex. Antimicrob Agents Chemother. 61(8):e02700–16. doi: 10.1128/AAC.02700-16.

Silva LG, Ferguson BS, Faciola AP. 2017. Rapid communication: prolactin and hydrocortisone impact TNFα-mediated mitogen-activated protein kinase signaling and inflammation of bovine mammary epithelial (MAC-T) cell. J Anim Sci. 95 (12):5524–5531. doi: 10.2527/jas2017.2028.

Sudbery PE. 2011. Growth of *Candida albicans* hyphae. Nat Rev Microbiol. 9(10):737–748. doi: 10.1038/nrmicro2636.

Tampakakis E, Okoli I, Mylonakis E. 2008. A *C. elegans*-based, whole animal, *in vivo* screen for the identification of antifungal compounds. Nat Protoc. 3(12):1925–1931. doi: 10.1038/nprot.2008.193.

Tan X, Fuchs BB, Wang Y, Chen W, Yuen GJ, Chen RB, Jayamani E, Anastassopoulou C, Pukkila-Worley R, Coleman JJ, et al. 2014. The role of *Candida albicans* SPT20 in filamentation, biofilm formation and pathogenesis. PLoS One. 9(4):e94468. doi: 10.1371/journal.pone.0094468.

Wang Y, Jia XM, Jia JH, Li MB, Cao YY, Gao PH, Liao WQ, Cao YB, Jiang YY. 2009. Ascorbic acid decreases the antifungal effect of fluconazole in the treatment of candidiasis. Clin Exp Pharmacol P. 36(10):e40–e46. doi: 10.1111/j.1440-1681.2009.05187.x.

Wu Y, Wu M, Wang Y, Chen Y, Gao J, Ying C. 2018. ERG11 couples oxidative stress adaptation, hyphal elongation and virulence in *Candida albicans*. FEMS Yeast Res. 18(7). doi: 10.1093/femsyr/foy057.

Xing XH, Wang XR, Chen L, Zhong H, Han L, Wang Y. 2023. Effect of MIR1 gene on the sensitivity of *Candida albicans* to azoles. Cent South Pharm. 21(5):1125–1129. doi: 10.7539/j.issn.1672-2981.2023.05.002.

Xu N, Dong YJ, Yu QL, Zhang B, Zhang M, Jia C, Chen YL, Zhang B, Xing LJ, Li MC. 2015. Convergent regulation of *Candida albicans* Aft2 and Czf1 in invasive and opaque filamentation. J Cell Biochem. 116(9):1908–1918. doi: 10.1002/jcb.25146.

Xu Y, Quan H, Wang Y, Zhong H, Sun J, Xu J, Jia N, Jiang Y. 2017. Requirement for ergosterol in berberine tolerance underlies synergism of fluconazole and berberine against fluconazole-resistant *Candida albicans* isolates. Front Cell Infect Microbiol. 7:491. doi: 10.3389/fcimb.2017.00491.

Xu Y, Wang Y, Yan L, Liang RM, Dai BD, Tang RJ, Gao PH, Jiang YY. 2009. Proteomic analysis reveals a synergistic mechanism of fluconazole and berberine against fluconazole-resistant *Candida albicans*: endogenous ROS augmentation. J Proteome Res. 8(11):5296–5304. doi: 10.1021/pr9005074.

Zara V, Dietmeier K, Palmisano A, Vozza A, Rassow J, Palmieri F, Pfanner N. 1996. Yeast mitochondria lacking the phosphate carrier/p32 are blocked in phosphate transport but can import preproteins after regeneration of a membrane potential. Mol Cell Biol. 16(11):6524–6531. doi: 10.1128/MCB.16.11.6524.